Article

Not peer-reviewed version

Estimating Position, Diameter at Breast Height, and Total Height of Eucalyptus Trees Using a PLS-SLAM

Milena Duarte Machado , Gilson Fernandes da Silva , André Quintão de Almeida , Adriano Ribeiro de Mendonça , Rorai Pereira Martins-Neto , Marcos Benedito Schimalski *

Posted Date: 22 July 2025

doi: 10.20944/preprints202507.1796.v1

Keywords: Mobile laser scanner; forest inventory; eucalyptus plantation

 doi:10.20944/preprints202507.1796.v1

Article

Estimating Position, Diameter at Breast Height, and Total Height of *Eucalyptus* Trees Using a PLS-SLAM

Milena Duarte Machado [1], Gilson Fernandes da Silva [1], André Quintão de Almeida [2], Adriano Ribeiro de Mendonça [1], Rorai Pereira Martins-Neto [3] and Marcos Benedito Schimalski [4,*]

[1] Department of Forest and Wood Sciences, Federal University of Espirito Santo, Jeronimo Monteiro, Espirito Santo, 29550-000, Brazil

[2] Department of Agricultural Engineering. Federal University of Sergipe, Saint Cristopher, Sergipe, 49.100-000, Brazil

[3] Faculty of Forestry and Wood Sciences, Czech University of Life Sciences Prague, Kamýcká 129, 16500 Prague, Czech Republic

[4] Department of Forestry Engineering, Center of Agroveterinary Sciences, Santa Catarina State University, Lages 89500000, SC, Brazil

* Correspondence: marcos.schimalski@udesc.br

Abstract

Forest management planning depends on accurately collecting information on available resources, gathered by forest inventories. However, due to the extent of the planted areas in Brazil, collecting information traditionally has become challenging. Based on the factors mentioned above, the objective of this study was to evaluate the accuracy of different point densities (points per square meter) in point clouds obtained through portable laser scanning combined with simultaneous localization and mapping (PLS-SLAM). The study aimed to identify tree positions and estimate the diameter at breast height (DBH) and total height (H) of 71 trees in a eucalyptus plantation in Brazil. The main findings indicate that denser point clouds (> 100 points.m-2) provided a more accurate representation of tree stems, successfully segmenting over 88.7% of the trees. The root mean square error (RMSE) of the best DBH measurement was 1.6 cm (5.9%) and of the best H measurement was 1.2 m (4.2%) for the point cloud with 36,000 returns.m-2. When measuring the total heights of the largest trees (H > 31.4 m) using LiDAR, the values were always underestimated considering a reference value, and their measurements were significantly different (p-value < 0.05 by the t-test). Point cloud degradation tended to reduce the accuracy of the DBH estimations, which was more evident in smaller trees (DBH ≤ 27.3 cm). In general, the degradation of the point cloud reduced the accuracy of the H estimates, which was more evident with larger trees (H > 31.4 m). Despite the reduction in accuracy in the conditions described above, we highlight the potential of PLS-SLAM to identify individuals in the plantation and estimate their main attributes.

Keywords: mobile laser scanner; forest inventory; eucalyptus plantation

1. Introduction

Brazil has an area with 9.93 million hectares of commercial plantations of implanted forests, with growth trends. Of this area, 75.8% are a fast-growing species—the genus Eucalyptus [1]. To manage this enormous forestry liability and with consideration for the most modern management models, detailed information on these plantations is needed in increasingly shorter time frames. This requires more accurate methods of forest inventory with lower costs and shorter durations.

Forest inventories are essential in any forestry company's management and decision-making processes, whether planting or native forests. Regarding planted forests, diameter at breast height (DBH) and total height (H) are commonly measured variables that are used in volumetric models to

 doi:10.20944/preprints202507.1796.v1

estimate the wood volume of trees, a difficult variable to estimate or obtain directly, especially in standing trees.

Measuring DBH is not a difficult task, and the available equipment that is currently used for this purpose, like calipers and diametric tapes, are easy to operate, low-cost and produces results with satisfactory accuracy [2]. However, regarding fixed area plots when conducting forest inventories, there is still a need to measure large numbers of individuals, which can make the work onerous and prone to errors due to fatigue of the field team. Measuring H is even more complicated; it is more expensive than measuring DBH and, in general, results in less accurate results. An alternative to the equipment commonly used by forestry companies is the use of regression models, which allows estimating the height based on DBH. Some heights are measured, and the remaining heights of the plot are estimated using hypsometric models. Many research papers have studied this [3–5], and recently, the use of machine learning techniques has produced accurate results [6,7].

The traditional way of conducting forest inventories—measuring DBH and H to estimate volume through volume tables or equations—has been the subject of several studies seeking more efficient ways to measure these variables. The most current research has examined active remote sensing tools, like light detection and ranging (LiDAR) sensors, to estimate these variables. LiDAR has been used to improve traditional forest inventories [8,9], accurately estimating the vegetation attributes at the area or individual tree level [2,10–13].

Although the use of LiDAR in forestry studies has expanded, the cost associated with these surveys remains high, especially for scanning large areas. LiDAR systems on manned aircraft have high operational costs. In contrast, systems using drones as the data collection platform have lower operational costs but are limited in range and payload capacity. Moreover, aerial LiDAR data typically do not allow for detailed representation of tree trunks. On the other hand, terrestrial LiDAR has limitations when applied to mapping large forested areas due to its static nature and restricted mobility. Additionally, the occlusion effect is one of the main limitations of using terrestrial LiDAR in forestry [12]. Therefore, Portable Laser Scanning (PLS) emerged with the potential to overcome the limitations of other laser scanning techniques. These tools can be carried by hand or in a backpack and used under any terrain condition, saving time in post-processing [14,15]. PLS has been successfully used to estimate the individual characteristics of trees [16–19]. However, PLS relies on high Global Navigation Satellite System (GNSS) coverage, which can be a limitation in densely forested areas. The development of PLS with simultaneous localization and mapping (PLS-SLAM) [20–23] allows real-time tree information collection and point cloud recording without the need of a GNSS system. Although sensors such as LiDAR are promising for measuring dendrometric variables of interest in forest inventories, many questions remain, limiting the popularization of this type of technology on an operational scale among forest-based companies, such as: Does this new paradigm present sufficiently accurate results? Is the time taken to obtain measurements significantly reduced? What is the ideal point cloud density? Is the cost of this new type of method offset by the results found? Is the level of detail of the information obtained, including the possibility of estimating the tree volume directly, advantageous in a new concept of forest management? The answers to these questions need more support and experiments to help us confidently confirm that the paradigm shift is indeed worthwhile.

Considering the issues raised about the use of LiDAR sensors to measure dendrometric variables, more specifically diameter at breast height (DBH) and height (H), the objective of this study is to evaluate the efficiency and accuracy of PLS-SLAM to identify the position of Eucalyptus trees and estimate the DBH and H of trees in different size classes under the influence of different point cloud densities.

 doi:10.20944/preprints202507.1796.v1

2. Materials and Methods

2.1. Study Area

This study was conducted in a *Eucalyptus grandis* stand located in the municipality of Jerônimo Monteiro (20º47'44.57" S, 41º24'19.72" W and 180 m altitude) in the state of Espírito Santo, southeast of Brazil (Figure 1). The area of the plot is approximately 417 m², with six planting rows containing 71 trees. The trees were numbered in ascending order, starting with the first individual in the first planting line. The stand was implanted in December 2010 in pits measuring 30 × 30 × 30 cm with a spacing of 3 × 2 m, using seedlings derived from seminal form.

The topography of the land is relatively flat (slope less than 1%), and the climate is classified as "Aw" (tropical) according to the Köppen-Geiger classification, with dry winters and rainy summers. The total annual precipitation is approximately 1,732 mm, and the average annual temperature is 24.6°C [24].

Figure 1. Localization of the study area.

2.2. Tradicional Forest Inventory

The observed DBH and H values of each tree in the stand were collected during two field campaigns. DBH values were measured with the aid of a Mantax Blues mechanical caliper manufactured by Haglof [25] and a wooden template 1.30 m high to ensure that the measurements were always performed at the same distance from the ground. Measurements were taken in two perpendicular positions and the average if these two measurements were taken.

The total height (H) of all trees in the plot was measured using a Leica TS02 total station [26] and a prism. While the distance between the equipment and each tree varied, efforts were made to maintain a horizontal distance equal to or greater than the tree's total height, due to the angle limitations of the equipment's observation lenses.

To measure H, the equipment was installed on a level tripod and positioned in a place with no obstacles between it and the prism, which was positioned next to the tree. The equipment generates a laser beam that is reflected by the prism and returned to the equipment, providing the horizontal distance between the equipment and the tree. Next, an upper view was taken at the highest point of the tree, and a lower view was taken at the base of the tree (Figure 2). When performing the upper

 doi:10.20944/preprints202507.1796.v1

and lower views, angles in degrees, minutes, and seconds were generated and noted in a field worksheet. To obtain the total heights of the trees, Equation 1 (presented below) was used:

$$H = \tan \alpha \, d + \tan \beta \, d \quad (1)$$

Where: H = total height, in meters (m), α = lower angle, in degrees (°), β = upper angle, in degrees (°), d = distance between the equipment and the tree, in meters (m).

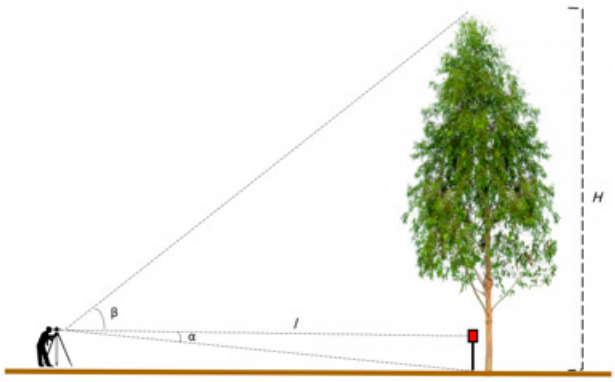

Figure 2. Schematic representation of how the total station was used to measure the total height of *E. grandis* trees in the field.

2.3. Portable Laser Scanning (PLS)

The evaluated plot was scanned using the PLS GeoSLAM ZEB-HORIZON 3D, model GS_510254 [27]. The weather was clear, with a wind speed of approximately 1.4 m.s^{-1} and an average air temperature of approximately 26° C. The ZEB-HORIZON is a lightweight PLS consisting of a Velodyne laser scanner working at a wavelength of 903 nm [27] and coupled to a motorized inertial measurement unit (IMU). The laser has an acquisition speed of 300,000 points.s^{-1} within a range of approximately 100 m around the instrument. It features 16 sensors, with a field of view of 270° × 360°, vertical and horizontal viewing angles of 2° and 0.38°, respectively, and a relative accuracy of ±6 mm depending on the environment.

The plot was scanned by one field operator (Figure 3). Before moving, the equipment was placed on a flat surface on the ground at the beginning of the plot (blue point in Figure 3). The PLS-SLAM was initialized and automatically calibrated, defining the point on the terrain surface as the origin of the initial coordinate system (ICS) in meters (x/y/z). The operator walked slowly (approximately 25 cm.s^{-1}) between the planting rows, holding the instrument approximately 1.4 m above the ground. The scanning time was approximately 6 minutes and 24 seconds. The average distance from the PLS to each tree was approximately 1.5 m. The path started and ended at the same point (blue point in Figure 3) and was carried out in a zigzag pattern.

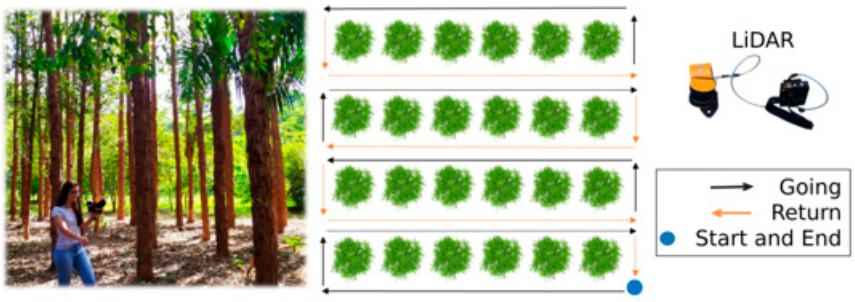

Figure 3. Representation of the path with the PLS-SLAM in the study area.

 doi:10.20944/preprints202507.1796.v1

The 3D point cloud was calculated from the raw data collected in the field and from the GeoSLam Hub server processing [27]. The application uses a SLAM system, which allows for the combination of the laser-scanning and the Inertial Measurement Unit (IMU) data to accurately generate 3D point clouds [12,20,21,28]. At the end of the process, a 3D cloud (.las) with approximately 65 million points was exported from the GeoSlam server. The point cloud was clipped using CloudCompare software version 2.6.1 [29], thus only the *E. grandis* plot with the trees of interest was considered in the next processing steps (Figure 4).

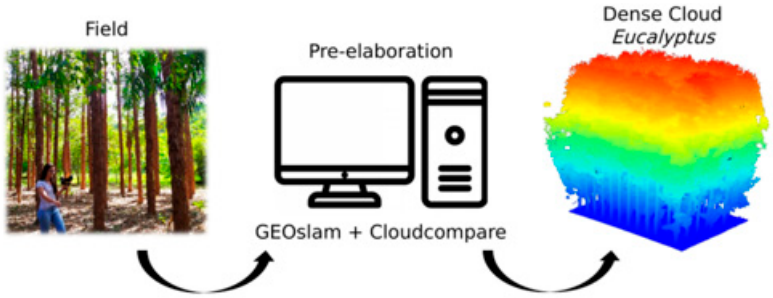

Figure 4. Steps to obtain the dense PLS-SLAM point cloud.

2.3.1. Resampling Point Clouds

To test the effect of different point densities on the estimation of forest parameters, the original point cloud (with a density of 36,000 returns.m^{-2}) was resampled to different densities: 1,000, 500, 100, and 10 returns.m^{-2}. The resampling was performed in R using the *decimate_points* function from the lidR package, creating a 3D grid with a 2-meter resolution and selecting 1,000, 500, 100, and 10 returns in each grid cell [30,31]. The accuracy of all estimates with degraded point clouds was evaluated to assess the influence of the number of returns per m² on the reduction of the accuracy of individual position estimates, as well as DBH and H values.

2.3.2. Automatic Tree Detection

The automatic detection of trees to estimate DBH and H values was performed based on the PLS-SLAM point clouds clipped for the planting area. All processing described below was performed with the help of functions available in the TreeLS [32] and lidR [30] packages for R enviroment, version 4.2.1 [31].

Initially, the classification of ground and non-ground points was performed using the cloth simulation filter (CSF) [33]. After preliminary tests, the best parameters were sloop smooth = TRUE, class threshold = 0.1, cloth resolution = 1, and time step = 0.5. Then, the digital terrain model (DTM) was constructed using the inverted distance weighing (IDW) of the points classified as ground with 1 m of spatial resolution. Then, the 3D point cloud was normalized (Figure 5).

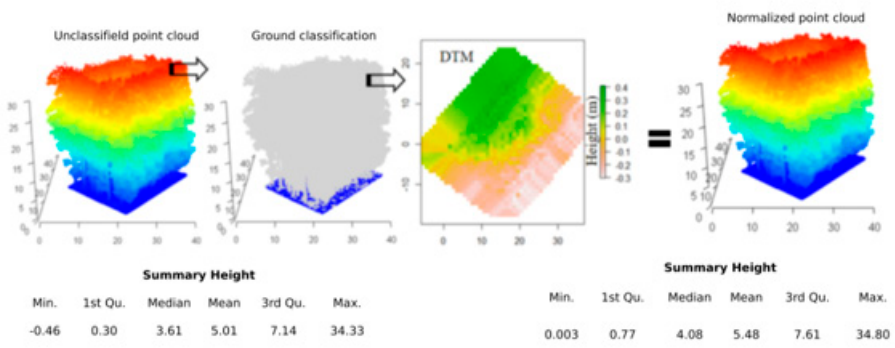

Figure 5. Representation of the stages of the normalization process of the dense point cloud through the classification of terrain points and generation of DTM.

 doi:10.20944/preprints202507.1796.v1

Next, the normalized cloud was resampled by a point sampling algorithm based on a systematic grid of voxels with a voxel length of 0.02 m (Figure 6a). The position (x/y) and identification of the stems were performed by Hough Transform, considering the minimum density value of points equal to 0.1 (Figure 6b). From the identified stems, the indexing and segmentation of each tree in the point cloud were performed (details of the segmentation in Figure 6c).

For segmentation, the Hough transformation algorithm considers a fixed circular radius from the position of the stem. To estimate DBH values, the radius of the circle was 1 m; to estimate H, it was 1.75 m. After segmenting the individuals, a classification of stem points was performed (with function *stemPoints*), considering Hough Transform as the noise removal method and extracting (with function *tlsInventory*) the values of DBH and H by fitting a circle to the stem with the Ransac algorithm [34,35] (red points in Figure 6d,e). More details about the adopted methodological flow can be found in the study developed by [32,36,37].

2.3.3. Automatic Tree Detection

Estimates of H values based on the existing semi-automatic method in the TreeLS package (with the *find_trees* function, [32]) were also evaluated, directly indicating the highest points of each previously segmented individual in the point cloud (detailed in Figure 6e).

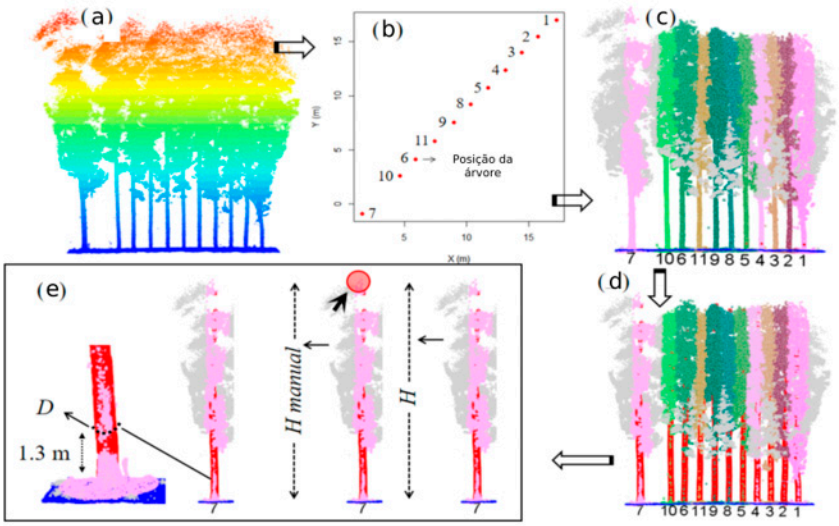

Figure 6. Detailing the segmentation and detection of individual trees automatically (a, b, c, d) and semi-automatic (e) to extract measurements from diameter at breast height (DBH) and total height (H).

2.4. Analysis of the DBH and H Estimations

To assess the accuracy of identifying tree stem positions according to each analyzed point cloud (36,000, 1,000, 500, 100, and 10 returns.m-2), the percentage of correct detections was calculated.

It is common, especially when estimating H using traditional measurement methods, for the size of a tree to influence the accuracy of the measurement. As a result, the sampled trees were divided into two size classes for both DBH and H, using the median as a reference for the division. To evaluate the estimates of DBH and H of the total number of trees and for the classes of trees correctly identified, the root mean square error (RMSE) and the relative and absolute bias were used, according to equations 2, 3, 4 and 5. The difference between the averages of the estimated values of DBH and H in the traditional and enhanced inventories was verified by the t-test for paired data (p-value < 0.05). The agreement between the data was evaluated using the determination coefficient (r^2).

$$RMSE = \sqrt{\frac{\sum_i^n (Y_i - \hat{Y}_i)^2}{n}} \quad (2)$$

 doi:10.20944/preprints202507.1796.v1

$$RMSE\ (\%) = \frac{RMSE}{\bar{Y}} 100 \quad (3)$$

$$Bias = \frac{\sum_i^n Y_i - \sum_i^n \hat{Y}}{n} \quad (4)$$

$$Bias\ (\%) = \frac{Bias}{\bar{Y}} 100 \quad (5)$$

Where: Y_i = diameter of the i-th tree obtained by the caliper (cm) and total height of the i-th tree obtained by the total station (m); $\hat{Y}_i$ = diameter estimated by PLS-SLAM of the i-th tree (cm) and total height estimated by PLS-SLAM of the i-th tree (m); $\bar{Y}$ = average diameter obtained by the caliper (cm) and average total height obtained by the total station (m); n = sample size (71 trees).

3. Results

3.1. Stem Detection

Figure 7 shows the map of the segmented tree stems and a 3D representation (Figure 7k) of one of the planting rows at the different densities of the points analyzed, selected at random to exemplify. The first line (Figure 7a–e) represents the stems identified for estimating DBH; the second (Figure 7f, 7g, 7h, 7i, and 7j) represents the segmented stems used for detecting H.

For DBH, the segmentation algorithm was able to identify the stems of all individuals (100%) in the point clouds of 36,000 and 1,000 returns.m^{-2} (Figure 7a,b). Only one individual was not identified in the point cloud of 500 and 100 returns.m^{-2} (Figure 7c,d). Regarding the cloud of 10 returns.m^{-2}, only 23.9% of individuals were detected (Figure 7e).

For H, it was also possible to identify the stems of 100% of the individuals in the point cloud of 36,000 returns.m^{-2} (Figure 7f) and 94.4% in the cloud of 1,000 returns.m^{-2} (Figure 7g). Of the trees, 88.7% were detected in the point clouds of 500 and 100 returns.m^{-2} (Figure 7h,i), while only 39.4% were detected in the point cloud with 10 returns.m^{-2} (Figure 7j).

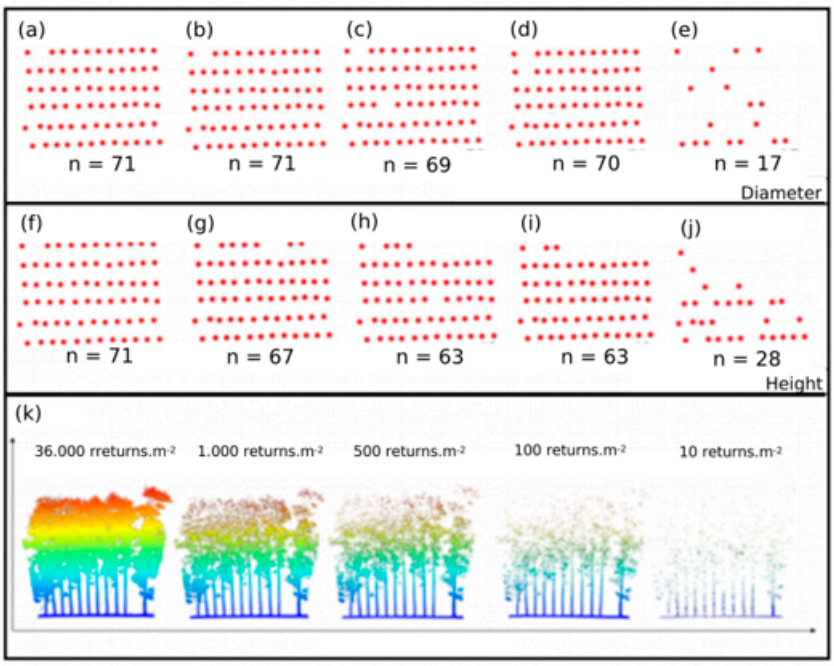

Figure 7. Position of *E. grandis* trees in the five different point cloud densities and profile of the first planting row in the five-point cloud densities.

 doi:10.20944/preprints202507.1796.v1

3.2. DBH Estimation

Regarding the total number of correctly identified trees, a tendency toward reduced accuracy was observed in a reduction in the density of points (Table 1). This reduction was not expressive up to a density of 100 returns.m^{-2} but became more evident at a density of 10 returns.m^{-2}. An exception to this trend was observed at a density of 1,000 returns.m^{-2}, which showed lower accuracy compared to the 500 and 100 returns.m^{-2} point clouds. The exact cause of this discrepancy was not identified. This pattern was consistent across both size classes.

However, accuracy was slightly higher for larger trees. It is also noteworthy that for a density of 10 returns.m^{-2}, there was a tendency to identify the largest trees more easily. This was evident when comparing the mean diameters of the caliper with those of the PLS-SLAM (Table 1). In Table 1, it can be seen that there was a slight tendency of the point clouds in all situations (All DBH, DBH ≤ 27.3 cm, and DBH > 27.3 cm) to underestimate DBH compared with the measurements obtained by the caliper.

Table 1. RMSE and Bias values for diameter at breast height (DBH) estimated by PLS-SLAM at different point cloud densities for *E. grandis* trees.

Returns	Diameter Class	N*	Mean		RMSE		BIAS	
			Caliper (cm)	PLS-SLAM (cm)	Abs (cm)	%	Abs (cm)	%
36,000	All DBH	71	27.8	26.5 (-4.67%)	1.6	5.9	1.3	4.8
1,000		71		26.2 (-5.75%)	2.4	9.3	1.7	5.9
500		70		26.4 (-5.03%)	1.9	6.8	1.5	5.5
100		70		26.4 (-5.03%)	2.1	7.4	1.5	5.2
10		17		31.5 (13,3%)	6.3	18.8	2.1	6.2
36,000	DBH ≤ 27.3 cm	35	21.3	20.1 (-5.63%)	1.6	7.3	1.3	5.9
1,000		35		20.1 (-5.63%)	2.3	10.6	1.3	6.0
500		33		20.1 (-5.63%)	1.6	7.4	1.2	5.7
100		34		20.2 (-5.16%)	1.8	8.7	1.0	4.5
10		3		25.8 (-21.1%)	5.7	22.2	0.0	-0.2
36,000	DBH > 27.3 cm	36	34.1	32.7 (-4.11%)	1.7	5.0	1.4	4.2
1,000		36		32.1 (-5.86%)	2.6	7.7	2.0	5.9
500		36		32.3 (-5.27%)	2.2	6.3	1.9	5.4
100		36		32.2 (-5.57%)	2.3	6.6	1.9	5.6
10		14		32.8 (-3.81%)	6.2	17.6	2.5	7.2

*N is the number of trees detected in the point cloud.

A high determination coefficient ($r^2 > 0.94$) between the values measured with the caliper and those estimated by the PLS-SLAM in the point clouds with 36,000, 1,000, 500, and 100 returns.m^{-2} and an intermediate determination coefficient ($r^2 = 0.51$) for the point cloud with 10 returns.m^{-2} can be observed in the results presented in Figure 8. It was also found that cloud dispersions with 36,000, 500, and 100 returns.m^{-2} were similar and had values close to the 1:1 line. The cloud dispersions of 1,000 and 10 returns.m^{-2} were farther from the 1:1 line (values below the line), making it clear that the PLS-SLAM measurements were underestimated in relation to the measures obtained by caliper.

Despite the underestimations verified in Table 1 and Figure 8, no significant differences were found (t-test for paired data, p-value > 0.05) between the caliper measurements and those estimated by the different point cloud densities (Figure 9). The exception was the point cloud with 10 returns.m^{-2}, which showed significant differences for all identified trees and for the case of class DBH ≤ 27.3 cm (Figure 9). It should be noted that in the case of All DBH, only 17 individuals were identified by the point cloud; in the case of DBH ≤ 27.3 cm, only three trees were identified.

From Figure 9, it can be inferred that the median values of the three situations evaluated, with the exception of the point cloud with 10 returns.m^{-2}, were close but slightly lower than the value found for the caliper. To a certain extent, this result corroborates the results in Table 1, emphasizing

 doi:10.20944/preprints202507.1796.v1

that the referred table evaluates mean values. Another relevant observation is the distribution of DBH, illustrated by the boxplot graph in Figure 9.

The distributions found for All DBH and DBH > 27.3 cm were similar in relation to the median position and occurrence of outliers. It should be emphasized that in the result found for All DBH, there was a greater coincidence of the caliper with the clouds evaluated between values below the interquartile compared to values above the interquartile. This reveals greater difficulty in estimating the diameters of the largest trees (DBH > 27.3 cm).

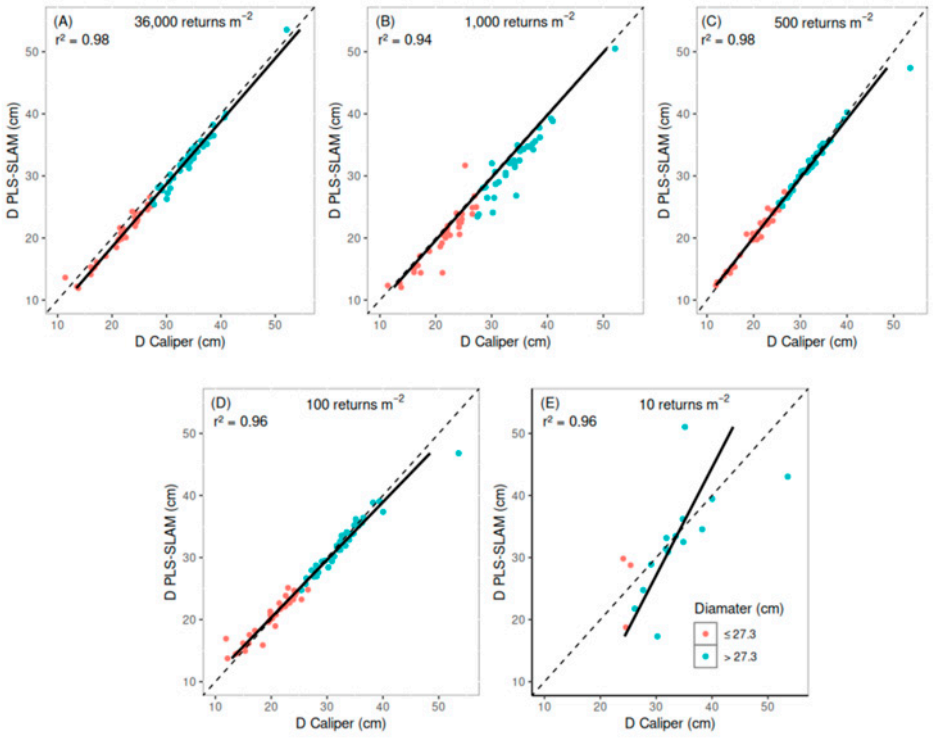

Figure 8. Scatter plots between the measurements of diameter at breast height (DBH) obtained by caliper and estimated by PLS-SLAM at different point densities for *E. grandis* trees.

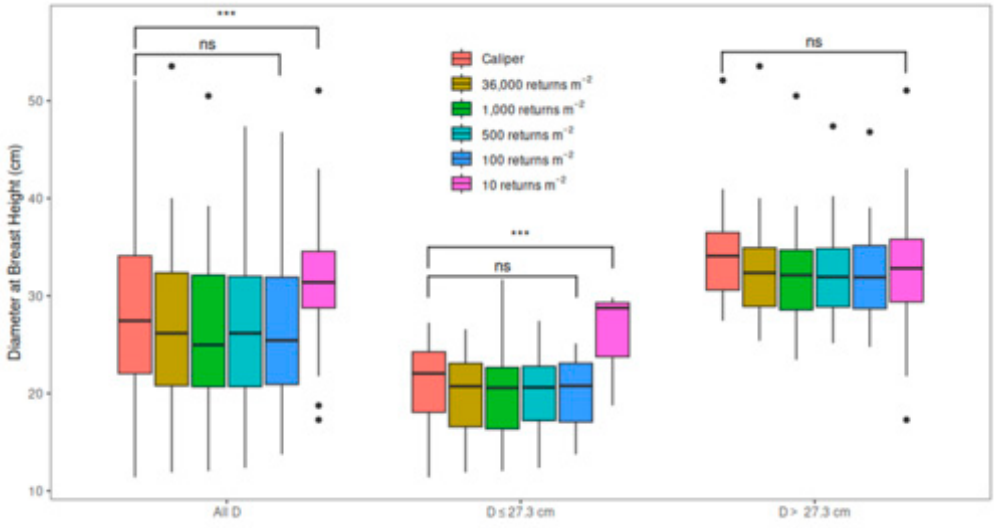

Figure 9. Boxplots of the diameter at breast height (DBH) estimated by the caliper and for five densities of point clouds generated by the PLS-SLAM, considering All DBH and the two diameter classes (DBH ≤ 27.3 cm e DBH > 27.3 cm). In the case of the t-test for paired data, ns = not significant (p-value > 0.05), *** = significant.

 doi:10.20944/preprints202507.1796.v1

3.3. Total Height Estimation

Regarding the total number of correctly identified trees, in both semi-automatic and automatic processing, a tendency toward reduced accuracy was observed via a reduction in the density of points (Table 2). This reduction was not expressive up to a density of 100 returns.m^{-2} but became more evident at a density of 10 returns.m^{-2}. This same behavior was observed for the two size classes in both processing methods, except in the H ≤ 31.4 m class of automatic processing, in which a high RMSE was observed in the five different point densities (ranging from 20.4% to 24.7%).

Regarding automatic processing, accuracy was higher for larger trees (H > 31.4 m). In semi-automatic processing, the two classes showed similar accuracy, with a clear trend of underestimating the H of the largest trees. However, in automatic processing, there was a slight tendency for point clouds in all situations to overestimate H.

Regarding semi-automatic processing, a high coefficient of determination ($r^2 > 0.93$) between total station and PLS-SLAM H values at densities of 36,000, 1,000, 500, and 100 returns.m^{-2} and a smaller coefficient of determination ($r^2 = 0.80$) for the cloud with 10 returns.m^{-2} were observed (Figure 10). In automatic processing, the r-square was intermediate (r^2 ranging from 0.63 to 0.67) for the point clouds with 36,000, 1,000, and 500 returns.m^{-2} and low ($r^2 = 0.39$) for the cloud of 100 returns.m^{-2}; there was a very low coefficient of determination ($r^2 = 0.05$) for the point cloud with 10 returns.m^{-2}. The dispersions for clouds of 36,000, 1,000, and 500 returns.m^{-2} in both processes and 100 returns.m^{-2} for automatic processing were similar (Figure 10). However, the dispersions in the point cloud of 10 returns.m^{-2} in both processes were farther from the 1:1 line, with values below the line, making it clear that the measures estimated by PLS-SLAM were underestimated concerning the measures obtained by the total station in the three situations (All H, H ≤ 31.4 m, and H > 31.4 m).

Table 2. Mean values of total height (H), RMSE, and bias regarding measurements obtained by the total station and estimated by PLS-SLAM, obtained semi-automatic and automatically, for different densities for *E. grandis* trees.

Returns	Total Height Class	N*	Mean		RMSE		BIAS	
			Total Station (m)	PLS-SLAM (m)	Abs (m)	%	Abs (m)	%
Automatic								
36,000	All H	71	29.5	30.9 (4.75%)	4.8	14.4	-1.4	-4.8
1,000		67		30.1 (2.03%)	4.0	13.7	1.2	4.0
500		63		29.6 (0.34%)	3.9	13.5	-0.1	-0.5
100		63		28.2 (-4.41%)	5.0	17.4	0.7	2.4
10		28		25.4 (-13.9%)	8.4	28.4	5.7	18.4
36,000	H ≤ 31.4 m	35	24.8	28.7 (15.7%)	5.9	23.8	-3.9	-15.7
1,000		34		27.8 (12.1%)	5.3	21.6	-3.1	-12.6
500		33		27.5 (10.9%)	5.1	20.4	-2.6	-10.4
100		34		25.9 (3.62%)	6.1	24.7	-1.2	-4.8
10		13		24.5 (-1.21%)	6.6	24.2	2.7	9.8
36,000	H > 31.4 m	36	34.0	33.0 (8.55%)	1.3	3.9	1.0	2.9
1,000		33		32.4 (6.58%)	1.8	5.3	1.6	4.7
500		30		32.0 (5.26%)	2.1	6.3	1.9	5.6
100		29		31.0 (1.97%)	3.4	9.9	2.9	8.6
10		15		26.1 (-14.15%)	9.7	28.2	8.4	24.3
semi-automatic								
36,000	All H	71	29.5	29.0 (-1.69%)	1.2	4.2	0.4	1.5
1,000				28.5 (-3.39%)	1.7	5.6	0.9	3.2
500				28.6 (-3.05%)	1.7	5.6	0.9	3.0
100				28.0 (-5.08%)	2.4	8.0	1.5	5.1
10				25.3 (-14.2%)	5.0	17.1	4.2	14.2

 doi:10.20944/preprints202507.1796.v1

36,000				25.1 (1.21%)	1.1	4.3	-0.3	-1.1
1,000				24.7 (-0.40%)	1.3	5.2	0.1	0.4
500	H ≤ 31.4 m	35	24.8	24.8 (-0.00%)	1.3	5.1	0.0	0.0
100				24.6 (-0.81%)	1.5	6.0	0.3	1.1
10				21.5 (-13.3%)	4.4	17.6	3.3	13.3
36,000				32.9 (-3.24%)	1.4	4.1	1.1	3.3
1,000				32.2 (-5.29%)	1.9	5.7	1.8	5.2
500	H > 31.4 m	36	34.0	32.2 (-5.29%)	2.0	5.8	1.8	5.2
100				31.3 (-7.94%)	3.0	8.7	2.7	8.0
10				28.9 (-15.0%)	5.6	16.4	5.1	14.9

*N is the number of trees detected in the point cloud.

Analyzing Figure 11A (automatic processing), no significant differences were found (t-test for paired data, p-value > 0.05) between the measurements obtained by the total station and those estimated by the point clouds with 36,000 and 1,000 returns.m^{-2} considering All H. For the two height classes, there were significant differences between the measurements obtained by the total station and those estimated by the different point cloud densities, except in the class of H ≤ 31.4 m for the clouds of 100 and 10 returns.m^{-2}.

In Figure 11B (semi-automatic processing), significant differences were not found (t-test for paired data, p-value > 0.05) between the measurements obtained by the total station and those estimated by the cloud with 36,000 returns.m^{-2} considering All H and for point clouds of 36,000, 1,000, 500, and 100 returns.m^{-2} in the class of H ≤ 31.4 m. The other clouds showed significant differences (t-test for paired data, p-value > 0.05).

In Figure 11, it can be observed that for All H and the class of H > 31.4 m, the PLS-SLAM underestimated the median value in both processing types. Concerning the class of H ≤ 31.4 m, in automatic processing, the median value was overestimated. For semi-automatic processing, there was an underestimation in point clouds with 1,000, 100, and 10 returns.m^{-2}. These results corroborate those in Table 2.

Also relevant is the distribution of H, illustrated by the boxplot graph in Figure 11. The distributions of All H and H > 31.4 m were similar regarding the median position and occurrence of outliers for both automatic and semi-automatic processing (Figure 11A,B). There was a greater occurrence of outliers for smaller trees in the classes of All H and H ≤ 31.4 m in automatic processing than in semi-automatic processing.

 doi:10.20944/preprints202507.1796.v1

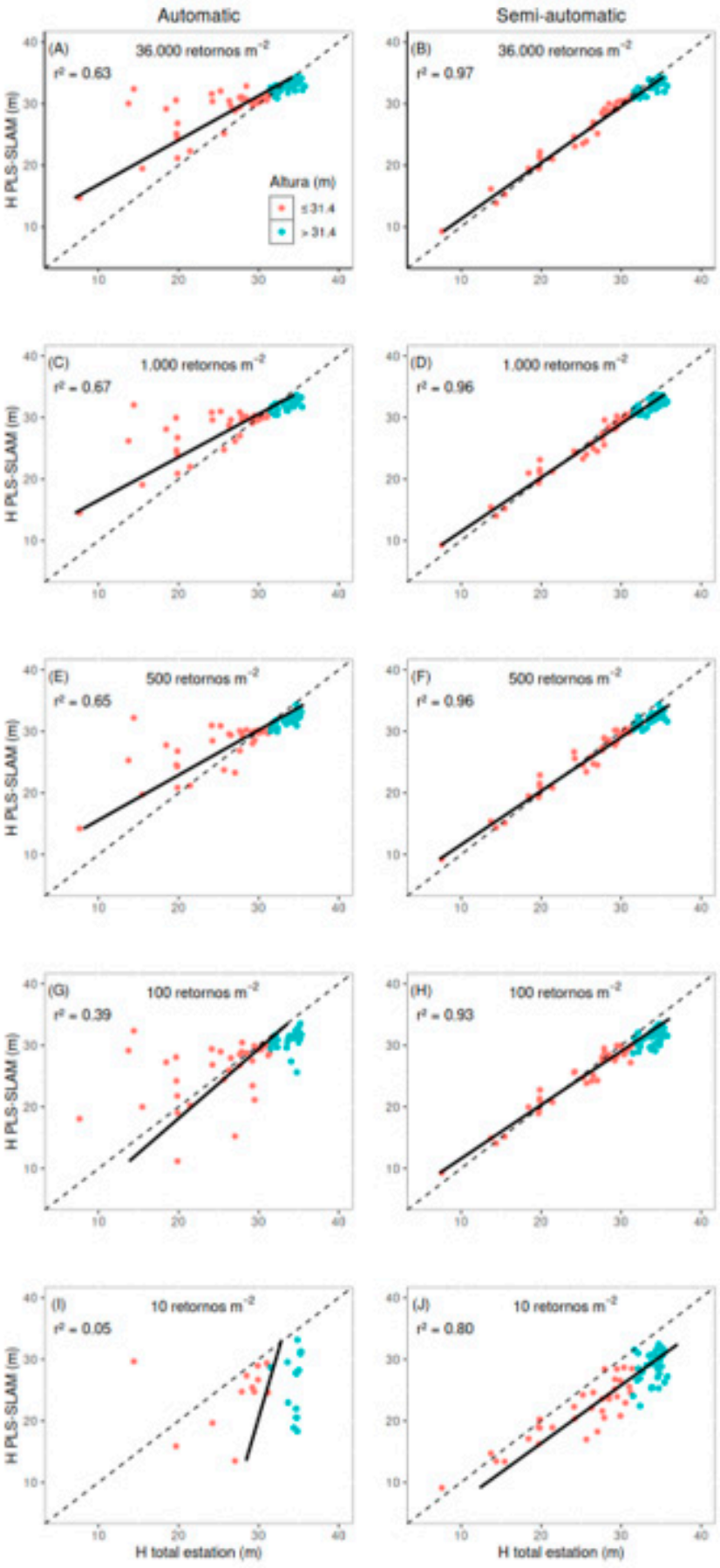

Figure 10. Scatter plots between total height (H) measurements obtained by the total station and estimated by PLS-SLAM, obtained semi-automatic and automatically at different point densities for *E. grandis* trees.

 doi:10.20944/preprints202507.1796.v1

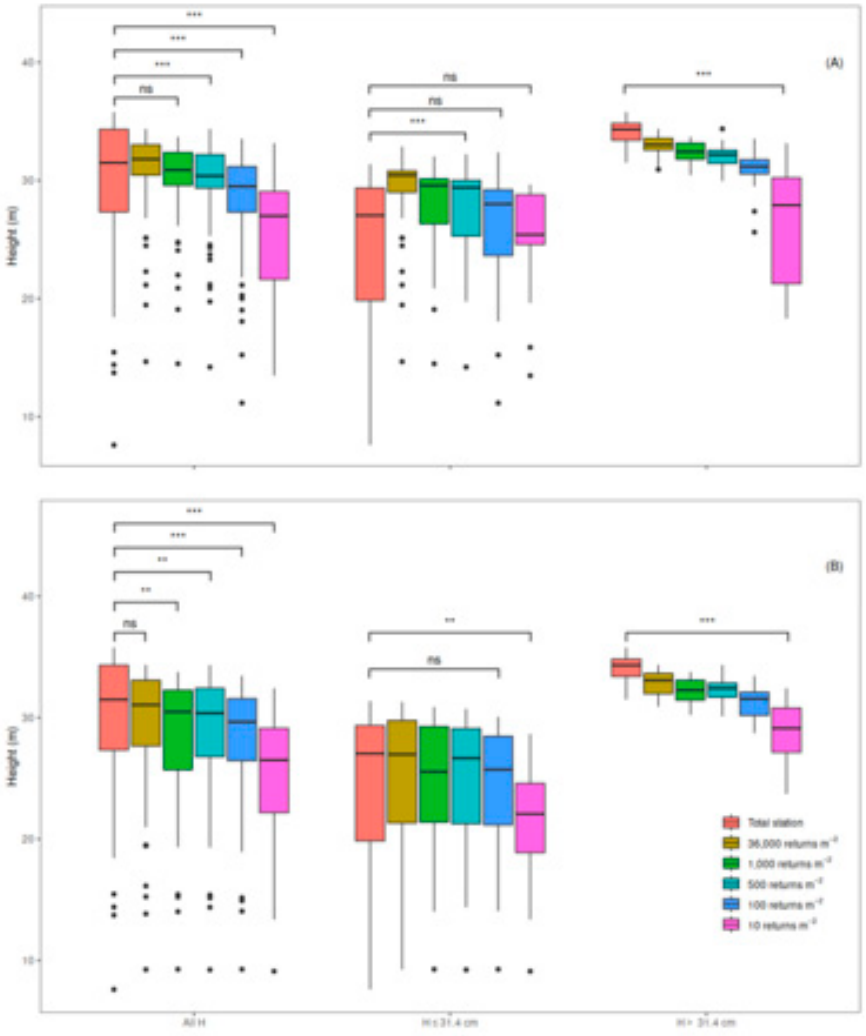

Figure 11. Boxplots of the total height (H) estimated by the total station and for the five different point cloud densities generated by PLS-SLAM, obtained automatically (A) and semi-automatic (B), considering All H and the two height classes (H ≤ 31.4 m and H > 31.4 m). In the case of the t-test for paired data, ns = not significant (p-value > 0.05), *** = significant.

4. Discussion

4.1. Stem Detection

Correct identification (segmentation) of the stem directly influences the quality of the results as well as the success of an improved forest inventory with PLS-SLAM data [11]. A good performance of the segmentation depends, among other factors, on the type of terrain, the typology and current conditions of the vegetation, the technical characteristics of the PLS, the type of path at the time of scanning, and the segmentation algorithm used [38]. In this study, during the stem segmentation process using the Ransac algorithm, it was observed that, regarding the radius of the circle equal to 1.0 meters, the H values of the trees were underestimated, which did not occur with the DBH values. The values of 1.0 and 1.75 m circle radius from the segmentation algorithm were used to estimate DBH and H, respectively.

In general, rates greater than 88.7% indicated good performance in the detection process of planting stems, except for the segmentation performed with the cloud of 10 returns.m^{-2} (less than a 39.4% detection rate). Ryding et al. (2015) [39] reported that a low density of cloud points and the existence of noise make it difficult to detect trees and increase the rate of unidentified individual

 doi:10.20944/preprints202507.1796.v1

trees. Despite the low detection rate of the point cloud with 10 returns.m^{-2}, the other point clouds achieved good segmentation results, with values greater than 90%, which is like what has been observed in other studies [14,15,40,41]. Some studies have reported difficulty detecting trees with smaller diameters [12,42], which was also observed in the present study.

When considering different circle radii in the segmentation algorithm, differences were observed in the detection rates of some analyzed point clouds (Tables 1 and 2 and Figure 7), mainly in the cloud with 10 returns.m^{-2}. These results show that, in addition to the density of the point cloud and the type of algorithm used, the values of its parameters influence the detection process.

4.2. DBH Estimation

The success of the stem segmentation process was essential to estimate DBH of the analyzed *Eucalyptus grandis* trees. The good results (RMSE < 7.4% and bias < 5.2%) found for the densest clouds (≥ 100 returns.m^{-2}) (Table 1, Figures 8 and 9) indicate the efficiency and accuracy of PLS-SLAM in estimating the DBH of the segmented trees, with similar, and even superior, performance [43,44] compared to other studies. Chiappini et al. (2022) [45] estimated the DBH of a *Pinus nigra* planted forest using a mobile laser scanner SLAM with RMSE values of 10.8%. Similarly, in analyzing a plantation of species of the genus *Pinus* in Finland, [46] reached an RMSE value of 14.63%.

Regarding the degradation of the point cloud, similar behaviors were observed, in terms of accuracy, among all the clouds, except for the point cloud of 10 returns.m^{-2}, which presented an inferior performance (Table 1, Figures 8 and 9). The point cloud of 1,000 returns.m^{-2} also stood out, presenting a slightly lower accuracy than the clouds of 500 and 100 returns.m^{-2}, especially for the smallest trees. No clear reason for this was found. This result is relevant insofar as less dense clouds correspond to less computational effort and greater ease of data processing, and assuming that accuracy is satisfactory, this may represent a great gain. For example, when purchasing a PLS-SLAM, the density of points needed to estimate the diameter does not necessarily need to be high, which can lead to the option of lower-cost equipment.

Although no significant reduction in accuracy was found with a reduction in point density in this study, [41] mentioned that a low density of points and the presence of noise directly influenced the estimates of trees in the smallest diameter classes; the largest errors occurred in trees with DBH ≤ 27.3 cm. This may be related to the segmentation algorithm used and its parameters, as the analysis used high density point clouds (36,000 and 1,000 returns.m^{-2}). Such RMSE values in the class of individuals with DBH ≤ 27.3 cm were also found by [39]; the authors reported an RMSE of 3.9 cm or 46%, which is significantly higher than the values found in this study six times greater (RMSE of 7.3%) than the percentage obtained for the cloud of 36,000 returns.m-2.

Lower RMSE and bias values were observed in the DBH > 27.3 cm class. The best performance (Table 1 and Figure 9) has also been reported in the estimations of trees with high diameter values in the literature [12,39,40,42]. This is a favorable result, since larger trees represent most of the volume or biomass, and a smaller error in larger trees therefore represents less error in the most significant portion thereof. This is relevant from the point of view of forest resource management.

In general, there was an underestimation of the DBH means in all point densities except the cloud with 10 returns.m^{-2}, in which there was an overestimation for All DBH and the class of DBH ≤ 27.3 cm. This was due to the low number of individuals segmented in this point cloud density. Gollob et al. (2020) [41] observed a trend of an underestimation of DBH increasing with the tree size, although this was not verified in this work.

4.3. Total Height Estimation

Height values are used to characterize the vertical structure of a forest or plantation and the quality of the site. In addition, they are input data for ecological models [47], forest fires [48], and growth and yield [49,50]. However, measurement difficulties and errors associated with their estimates are greater. Therefore, the use of accurate methods with high performance levels and reduced costs is desirable for estimating H during a forest inventory. Despite its importance, few

 doi:10.20944/preprints202507.1796.v1

studies have evaluated the accuracy of H estimates performed using PLS-SLAM [15,45,51], and these have mainly been in forest formations of fast-growing species.

As described, H estimates were performed in two ways: automatically, via segmentation, and semi-automatic, indicating the top of the tree directly over the point cloud. Regarding the automatic processing, the most relevant result (Table 2) was a considerable reduction in accuracy for smaller trees, which did not occur for larger trees. This can largely be explained by the difficulty of the segmentation algorithm used to identify the tops of the smallest trees; the algorithm considers maximum height, which in most cases refers to the stems, branches, and crowns of neighboring trees of the upper stratum. However, concerning All H, the results of this study were similar to those of [45] (RMSE of 10.2% and bias of -0.7%) when estimating the H (between 15 and 35 m) of trees on a coniferous plantation with a mobile mapping system in central Italy.

When the H estimation was performed semi-automatically, a significant increase in accuracy was noted, with a reduction in RMSE and bias, especially for trees with H ≤ 31.4 m (Table 2). This occurred because, in semi-automatic processing, the measurer can indicate the H of a tree more assertively. As mentioned, the algorithm that performs the automatic segmentation will likely confuse the tops with the stems, branches, and crowns of larger neighboring trees, especially with the smallest trees. Semi-automatic processing requires more time to measure the same number of trees; thus, it is less efficient. In this sense, the search for more accurate segmentation methods should be a continued object of investigation.

It should be noted that this work did not aim to test different segmentation algorithms, but this would undoubtedly be a valuable consideration for future work. Regarding the use of automatic processing only, [15] did not recommend the use of PLS-SLAM to estimate height values > 25 m for different conditions in a boreal forest in Finland. However, the author did not test any type of semi-automatic processing, and the results found in the current study indicate that in the absence of a good segmentation algorithm, semi-automatic processing can be a viable alternative.

It is important to consider that the range, pulse width (T0), scanning range, and laser acquisition rate influence the accuracy of a measurement [15]. The PLS-SLAM laser used in this study has a T0 of 6 ns, an acquisition speed of 300,000 points.s^{-1}, an approximate range of 100 m, 16 sensors, and a 270° x 360° field of view. It was not the objective of this study to evaluate the influence of these characteristics on the accuracy of H measurements. However, in future works, it is worth evaluating the hypothesis of the influence of T0 and the field of vertical view (270°) as a possibles factors of underestimation of H for larger trees.

Despite the error analyses comparing H measurements obtained by the PLS-SLAM with the total station, the total station was considered the reference H. It is important to highlight that the measurement obtained by the total station may also be subject to error, as it is an indirect measurement method. Ideally, the trees evaluated should be felled to obtain more reliable height values, which is not an easy task, often unauthorized. In addition, the structure and complexity of planting, tree height, and human error, among other factors [38,52], can influence the occurrence of errors. Therefore, measurement uncertainties and the propagation of errors should also be the focus of future research.

In summary, adequate forest management planning depends directly on the collection of accurate information about available resources through forest inventories [53]. In traditional inventories, the total height of a tree and its diameter at breast height are the attributes of greatest interest [54], along with wood volume, site indices, and biomass estimation [19]. However, estimating this information in the field requires great physical and operational effort and is costly, especially when repeated measurements are required over time [2]. In addition to obtaining reliable estimates of the forest's dendrometric variables of interest [15,38,44], the effort and cost are considerably reduced when using PLS-SLAM data, especially for full height measurements [45].

 doi:10.20944/preprints202507.1796.v1

5. Conclusions

This study demonstrated the potential of PLS-SLAM technology for estimating dendrometric variables in *Eucalyptus* plantations. Point clouds with densities above 100 returns.m^{-2} enabled accurate individual tree segmentation and reliable estimates of diameter at breast height (DBH) and total height (H). However, resampling to lower point clouds densities tended to reduce the accuracy of DBH estimates, particularly for smaller trees (DBH ≤ 27.3 cm). Similarly, a decrease in point density negatively impacted the accuracy of height estimates, with more pronounced errors observed in taller trees (H > 31.4 m).

Semi-automatic processing provided significantly better height estimation results than fully automatic methods, especially for smaller trees. Nevertheless, its application on a large scale may be limited by reduced efficiency, potentially affecting overall accuracy. Despite these limitations, the findings highlight the feasibility of using PLS-SLAM as a practical tool for forest inventory applications, balancing accuracy and operational efficiency, and supporting more detailed forest resource assessments.

Author Contributions: Conceptualization, M.D.M., G.F.S. and A.Q.A.; methodology, M.D.M., G.F.S., A.Q.A., A.R.M., R.P.M.N. and M.B.S.; software, M.D.M., A.Q.A. and R.P.M.N.; validation, M.D.M., G.F.S., A.Q.A. and A.R.M.; formal analysis, M.D.M., G.F.S., A.Q.A., A.R.M., R.P.M.N. and M.B.S.; investigation, M.D.M., G.F.S., A.Q.A. and A.R.M.; resources, G.F.S., A.Q.A. and A.R.M.; data curation, M.D.M., G.F.S., A.Q.A. and R.P.M.N.; writing—original draft preparation, M.D.M.; writing—review and editing, M.D.M., G.F.S., A.Q.A., A.R.M., R.P.M.N. and M.B.S.; visualization, M.D.M., A.Q.A. and M.B.S.; supervision, G.F.S., A.Q.A and A.R.M.; project administration, G.F.S., A.Q.A and A.R.M.; funding acquisition, G.F.S. and A.Q.A. All authors have read and agreed to the published version of the manuscript.

Funding: This research received no external funding.

Data Availability Statement: Data is available upon request to the authors.

Acknowledgments: This Project would not have been possible without the support of the Forest Management and Measurement Laboratory at the Federal University of Espírito Santo. The authors would like to thank CNPq for the research grant from the author André Q. Almeida of the project "TREEcarbon: Remote forest carbon monitoring system for the Atlantic Forest and Caatinga Biomes" process 300234/2022-8. The author Rorai Pereira Martins-Neto was partially founded by the grant FORESTin3D.

Conflicts of Interest: The authors declare no conflicts of interest.

Abbreviations

The following abbreviations are used in this manuscript:

CSF	Cloth Simulation Filter
DBH	Diameter at breast height
GNSS	Global Navigation Satellite System
H	Total height
ICS	Initial Coordinate System
IMU	Inertial Measurement Unit
LiDAR	Light Detection and Ranging
PLS	Portable Laser Scanner
RMSE	Root-mean square error
SLAM	Simultaneous Localization and Mapping

References

1. IBÁ, I.B. de Á. IBÁ Annual Report 2022.

2. Shao, J.; Zhang, W.; Mellado, N.; Wang, N.; Jin, S.; Cai, S.; Luo, L.; Lejemble, T.; Yan, G. SLAM-Aided Forest Plot Mapping Combining Terrestrial and Mobile Laser Scanning. *ISPRS Journal of Photogrammetry and Remote Sensing* **2020**, *163*, 214–230, doi:https://doi.org/10.1016/j.isprsjprs.2020.03.008.
3. Acosta, H.A.B.; Garrett, A.T. de A.; Lanssanova, L.R.; Dias, A.N.; Tambarussi, E.V.; Filho, A.F.; Guimarães, F.A.R.; Cabral, O.M.V. Identity of Hypsometric Models for Eucalyptus Clones in the Eastern Region of Paraguay. **2020**, *48*, 12, doi:https://doi.org/10.18671/scifor.v48n125.16.
4. Carielo, P.; Arce, J.E.; Figueiredo Filho, A.; Pelissari, A.L.; Kohler, S.V.; Retslaff, F.A. de S.; Behling, A. Agrupamento de Dados Para Ajustes de Modelos Hipsométricos e Volumétricos Em Povoamentos de Pinus Oocarpa e Pinus Caribaea Var. Hondurensis. *Ciência Florestal* **2022**, *32*, 1165–1186, doi:https://doi.org/10.5902/1980509835017.
5. Stolle, L.; Velozo, D.R.; Corte, A. dalla; Sanquetta, R.C.; Beutling, A. Hypsometric Models for a Khaya Ivorensis a. Chev Young Stand. **2018**, *3*, 6, doi:dx.doi.org/10.5380/biofix.v3i2.58799.
6. de Oliveira Valente, E.; Valente, G. de F.S. Simulação de Redes Neurais Artificiais Para Estimativa de Volume de Madeira Florestal a Partir Do DAP. *Brazilian Journal of Animal and Environmental Research* **2021**, *4*, 3748–3757, doi:https://doi.org/10.34188/bjaerv4n3-080.
7. Martins, A.P.M.; Debastiani, A.B.; Pelissari, A.L.; Machado, S. do A.; Sanquetta, C.R. Estimativa Do Afilamento Do Fuste de Araucária Utilizando Técnicas de Inteligência Artificial. *Floresta e Ambiente* **2017**, *24*, e20160234, doi:https://doi.org/10.1590/2179-8087.023416.
8. Pierzchała, M.; Giguère, P.; Astrup, R. Mapping Forests Using an Unmanned Ground Vehicle with 3D LiDAR and Graph-SLAM. *Computers and Electronics in Agriculture* **2018**, *145*, 217–225, doi:https://doi.org/10.1016/j.compag.2017.12.034.
9. Mokroš, M.; Výbošťok, J.; Tomaštík, J.; Grznárová, A.; Valent, P.; Slavík, M.; Merganič, J. High Precision Individual Tree Diameter and Perimeter Estimation from Close-Range Photogrammetry. *Forests* **2018**, *9*, 696, doi:https://doi.org/10.3390/f9110696.
10. Pyörälä, J.; Kankare, V.; Liang, X.; Saarinen, N.; Rikala, J.; Kivinen, V.-P.; Sipi, M.; Holopainen, M.; Hyyppä, J.; Vastaranta, M. Assessing Log Geometry and Wood Quality in Standing Timber Using Terrestrial Laser-Scanning Point Clouds. *Forestry: An International Journal of Forest Research* **2019**, *92*, 177–187, doi:https://doi.org/10.1093/forestry/cpy044.
11. Liang, X.; Kukko, A.; Hyyppä, J.; Lehtomäki, M.; Pyörälä, J.; Yu, X.; Kaartinen, H.; Jaakkola, A.; Wang, Y. In-Situ Measurements from Mobile Platforms: An Emerging Approach to Address the Old Challenges Associated with Forest Inventories. *ISPRS Journal of Photogrammetry and Remote Sensing* **2018**, *143*, 97–107, doi:https://doi.org/10.1016/j.isprsjprs.2018.04.019.
12. Bauwens, S.; Bartholomeus, H.; Calders, K.; Lejeune, P. Forest Inventory with Terrestrial LiDAR: A Comparison of Static and Hand-Held Mobile Laser Scanning. *Forests* **2016**, *7*, 127, doi:https://doi.org/10.3390/f7060127.
13. Wulder, M.A.; Coops, N.C.; Hudak, A.T.; Morsdorf, F.; Nelson, R.; Newnham, G.; Vastaranta, M. Status and Prospects for LiDAR Remote Sensing of Forested Ecosystems. *Canadian Journal of Remote Sensing* **2013**, *39*, S1–S5, doi:10.5589/m13-051.
14. Chen, S.; Liu, H.; Feng, Z.; Shen, C.; Chen, P. Applicability of Personal Laser Scanning in Forestry Inventory. *PLoS One* **2019**, *14*, e0211392, doi:https://doi.org/10.1371/journal.pone.0211392.
15. Hyyppä, E.; Kukko, A.; Kaijaluoto, R.; White, J.C.; Wulder, M.A.; Pyörälä, J.; Liang, X.; Yu, X.; Wang, Y.; Kaartinen, H. Accurate Derivation of Stem Curve and Volume Using Backpack Mobile Laser Scanning. *ISPRS Journal of Photogrammetry and Remote Sensing* **2020**, *161*, 246–262, doi:https://doi.org/10.1016/j.isprsjprs.2020.01.018.
16. Piermattei, L.; Karel, W.; Wang, D.; Wieser, M.; Mokroš, M.; Surovỳ, P.; Koreň, M.; Tomaštík, J.; Pfeifer, N.; Hollaus, M. Terrestrial Structure from Motion Photogrammetry for Deriving Forest Inventory Data. *Remote Sensing* **2019**, *11*, 950, doi:https://doi.org/10.3390/rs11080950.
17. Liang, X.; Kankare, V.; Hyyppä, J.; Wang, Y.; Kukko, A.; Haggrén, H.; Yu, X.; Kaartinen, H.; Jaakkola, A.; Guan, F. Terrestrial Laser Scanning in Forest Inventories. *ISPRS Journal of Photogrammetry and Remote Sensing* **2016**, *115*, 63–77, doi:https://doi.org/10.1016/j.isprsjprs.2016.01.006.

 doi:10.20944/preprints202507.1796.v1

18. Brede, B.; Calders, K.; Lau, A.; Raumonen, P.; Bartholomeus, H.M.; Herold, M.; Kooistra, L. Non-Destructive Tree Volume Estimation through Quantitative Structure Modelling: Comparing UAV Laser Scanning with Terrestrial LIDAR. *Remote Sensing of Environment* **2019**, *233*, 111355, doi:https://doi.org/10.1016/j.rse.2019.111355.
19. Liu, G.; Wang, J.; Dong, P.; Chen, Y.; Liu, Z. Estimating Individual Tree Height and Diameter at Breast Height (DBH) from Terrestrial Laser Scanning (TLS) Data at Plot Level. *Forests* **2018**, *9*, 398, doi:https://doi.org/10.3390/f9070398.
20. Durrant-Whyte, H.; Bailey, T. Simultaneous Localization and Mapping: Part I. *IEEE robotics & automation magazine* **2006**, *13*, 99–110.
21. Bailey, T.; Durrant-Whyte, H. Simultaneous Localization and Mapping (SLAM): Part II. *IEEE robotics & automation magazine* **2006**, *13*, 108–117.
22. Qian, C.; Liu, H.; Tang, J.; Chen, Y.; Kaartinen, H.; Kukko, A.; Zhu, L.; Liang, X.; Chen, L.; Hyyppä, J. An Integrated GNSS/INS/LiDAR-SLAM Positioning Method for Highly Accurate Forest Stem Mapping. *Remote Sensing* **2016**, *9*, 3.
23. Zhang, J.; Singh, S. LOAM: Lidar Odometry and Mapping in Real-Time. In Proceedings of the Robotics: Science and systems; Berkeley, CA, 2014; Vol. 2, pp. 1–9.
24. INCAPER, I.C. de P., Assistência Técnica e Extensão Rural Programa de Assistência Técnica e Rural Jerônimo Montero (PROATER 2020 - 2023). 2020.
25. Haglöf Sweden Haglöf Mantax Blue Caliper 2021.
26. Leica Geosystems Leica FlexLine TS02plus - Data Sheet 2022.
27. GeoSLAM ZEB HORIZON The Ultimate Mobile Mapping Solution 2022.
28. GeoSLAM What Is SLAM (Simultaneous Localisation and Mapping)? 2022.
29. CloudCompare, G. CloudCompare 2022.
30. Roussel, J.-R.; Auty, D. lidR: Airborne LiDAR Data Manipulation and Visualization for Forestry Applications. R Package Version 3.1.4 2022.
31. R Core Team R: The R Project for Statistical Computing 2022.
32. De Conto, T. TreeLS: Terrestrial Point Cloud Processing of Forest Data 2022.
33. Zhang, W.; Qi, J.; Wan, P.; Wang, H.; Xie, D.; Wang, X.; Yan, G. An Easy-to-Use Airborne LiDAR Data Filtering Method Based on Cloth Simulation. *Remote sensing* **2016**, *8*, 501, doi:https://doi.org/10.3390/rs8060501.
34. Olofsson, K.; Holmgren, J.; Olsson, H. Tree Stem and Height Measurements Using Terrestrial Laser Scanning and the RANSAC Algorithm. *Remote sensing* **2014**, *6*, 4323–4344, doi:https://doi.org/10.3390/rs6054323.
35. Tittmann, P.; Shafii, S.; Hartsough, B.; Hamann, B. Tree Detection and Delineation from LiDAR Point Clouds Using RANSAC. *Proceedings of SilviLaser* **2011**, 1–23.
36. de Conto, T.; Olofsson, K.; Görgens, E.B.; Rodriguez, L.C.E.; Almeida, G. Performance of Stem Denoising and Stem Modelling Algorithms on Single Tree Point Clouds from Terrestrial Laser Scanning. *Computers and Electronics in Agriculture* **2017**, *143*, 165–176, doi:https://doi.org/10.1016/j.compag.2017.10.019.
37. Heinzel, J.; Huber, M.O. Tree Stem Diameter Estimation from Volumetric TLS Image Data. *Remote Sensing* **2017**, *9*, 614, doi:https://doi.org/10.3390/rs9060614.
38. Balenović, I.; Liang, X.; Jurjević, L.; Hyyppä, J.; Seletković, A.; Kukko, A. Hand-Held Personal Laser Scanning–Current Status and Perspectives for Forest Inventory Application. *Croatian Journal of Forest Engineering: Journal for Theory and Application of Forestry Engineering* **2021**, *42*, 165–183, doi:https://doi.org/10.5552/crojfe.2021.858.
39. Ryding, J.; Williams, E.; Smith, M.J.; Eichhorn, M.P. Assessing Handheld Mobile Laser Scanners for Forest Surveys. *Remote sensing* **2015**, *7*, 1095–1111, doi:https://doi.org/10.3390/rs70101095.
40. Cabo, C.; Del Pozo, S.; Rodríguez-Gonzálvez, P.; Ordóñez, C.; González-Aguilera, D. Comparing Terrestrial Laser Scanning (TLS) and Wearable Laser Scanning (WLS) for Individual Tree Modeling at Plot Level. *Remote Sensing* **2018**, *10*, 540, doi:https://doi.org/10.3390/rs10040540.

 doi:10.20944/preprints202507.1796.v1

41. Gollob, C.; Ritter, T.; Nothdurft, A. Forest Inventory with Long Range and High-Speed Personal Laser Scanning (PLS) and Simultaneous Localization and Mapping (SLAM) Technology. *Remote Sensing* **2020**, *12*, 1509, doi:https://doi.org/10.3390/rs12091509.
42. Giannetti, F.; Puletti, N.; Quatrini, V.; Travaglini, D.; Bottalico, F.; Corona, P.; Chirici, G. Integrating Terrestrial and Airborne Laser Scanning for the Assessment of Single-Tree Attributes in Mediterranean Forest Stands. *European Journal of Remote Sensing* **2018**, *51*, 795–807, doi:10.1080/22797254.2018.1482733.
43. Zhou, T.; Popescu, S.C. Bayesian Decomposition of Full Waveform LiDAR Data with Uncertainty Analysis. *Remote sensing of environment* **2017**, *200*, 43–62, doi:https://doi.org/10.1016/j.rse.2017.08.012.
44. Vatandaşlar, C.; Zeybek, M. Application of Handheld Laser Scanning Technology for Forest Inventory Purposes in theNE Turkey. *Turkish Journal of Agriculture and Forestry* **2020**, *44*, 229–242, doi:10.3906/tar-1903-40.
45. Chiappini, S.; Pierdicca, R.; Malandra, F.; Tonelli, E.; Malinverni, E.S.; Urbinati, C.; Vitali, A. Comparing Mobile Laser Scanner and Manual Measurements for Dendrometric Variables Estimation in a Black Pine (Pinus Nigra Arn.) Plantation. *Computers and Electronics in Agriculture* **2022**, *198*, 107069, doi:https://doi.org/10.1016/j.compag.2022.107069.
46. Liang, X.; Kukko, A.; Kaartinen, H.; Hyyppä, J.; Yu, X.; Jaakkola, A.; Wang, Y. Possibilities of a Personal Laser Scanning System for Forest Mapping and Ecosystem Services. *Sensors* **2014**, *14*, 1228–1248, doi:https://doi.org/10.3390/s140101228.
47. Reyes-Ramos, A.; Cruz de León, J.; Martínez-Palacios, A.; Lobit, P.C.M.; Ambríz-Parra, J.E.; Sánchez-Vargas, N.M. Ecological and Dendrometric Characters in Which Influence Resin Production of Pinus Oocarpa of Michoacán, Mexico. *Madera y bosques* **2019**, *25*, doi:https://doi.org/10.21829/myb.2019.2511414.
48. Toalombo, J.C.; Salguero, M.; Criollo, E.C. Valoración Social Económica Ambiental de Los Incendios Forestales. **2021**, doi:https://doi.org/10.33996/revistaalfa.v5i15.142.
49. Penido, T.M.A.; Lafetá, B.O.; Nogueira, G.S.; Alves, P.H.; Gorgens, E.B.; de Oliveira, M.L.R. Growth and Production Models for Volumetric Estimates in Commercial Eucalypt Stands. *Scientia Forestalis* **2020**, *48*, 12, doi:10.18671/scifor.v48n128.06.
50. Landsberg, J.J.; Waring, R.H. A Generalised Model of Forest Productivity Using Simplified Concepts of Radiation-Use Efficiency, Carbon Balance and Partitioning. *Forest ecology and management* **1997**, *95*, 209–228, doi:https://doi.org/10.1016/S0378-1127(97)00026-1.
51. Jurjević, L.; Liang, X.; Gašparović, M.; Balenović, I. Is Field-Measured Tree Height as Reliable as Believed–Part II, A Comparison Study of Tree Height Estimates from Conventional Field Measurement and Low-Cost Close-Range Remote Sensing in a Deciduous Forest. *ISPRS Journal of Photogrammetry and Remote Sensing* **2020**, *169*, 227–241, doi:https://doi.org/10.1016/j.isprsjprs.2020.09.014.
52. Stereńczak, K.; Mielcarek, M.; Wertz, B.; Bronisz, K.; Zajączkowski, G.; Jagodziński, A.M.; Ochał, W.; Skorupski, M. Factors Influencing the Accuracy of Ground-Based Tree-Height Measurements for Major European Tree Species. *Journal of environmental management* **2019**, *231*, 1284–1292, doi:https://doi.org/10.1016/j.jenvman.2018.09.100.
53. Müller, A.; Olschewski, R.; Unterberger, C.; Knoke, T. The Valuation of Forest Ecosystem Services as a Tool for Management Planning–A Choice Experiment. *Journal of environmental management* **2020**, *271*, 111008, doi:https://doi.org/10.1016/j.jenvman.2020.111008.
54. Wang, Y.; Lehtomäki, M.; Liang, X.; Pyörälä, J.; Kukko, A.; Jaakkola, A.; Liu, J.; Feng, Z.; Chen, R.; Hyyppä, J. Is Field-Measured Tree Height as Reliable as Believed–A Comparison Study of Tree Height Estimates from Field Measurement, Airborne Laser Scanning and Terrestrial Laser Scanning in a Boreal Forest. *ISPRS journal of photogrammetry and remote sensing* **2019**, *147*, 132–145, doi:https://doi.org/10.1016/j.isprsjprs.2018.11.008.